

# Momentum Correlations in Nuclear Collisions

By: Patrick Carzon

Advisors: Sean Gavin, George Moschelli

August 2016

## 1 Introduction

Covariance is a measure of how linearly two things change with each other. Here we look at the covariance of the momentums of particles created by nuclear collisions. This covariance is used to calculate the viscosity of the Quark Gluon Plasma created by these nuclear collisions.<sup>1</sup> The covariance in ref. (1) uses transverse momentum and here we look at Cartesian momentum as a further source of insight. In order to do this, we analyze Au on Au collisions at  $\sqrt{s} = 200\text{GeV}$  produced by the simulation engine AMPT and compare our results to data produced by STAR<sup>2</sup> to ensure accuracy.

### 1.1 Particle Momentum

Transverse momentum, particle momentum perpendicular to the beam direction,  $p_t$ , is the standard measurement. This has given us much insight into the viscosity of QGP and has helped shape our understanding of this form of matter. We decided to expand on this understanding by looking at momentum correlations with respect to Cartesian momentum coordinates. This is significant because momentum in  $x$  and  $y$  are conserved when all particles are included while transverse momentum is not. This is easily seen by the definition of  $p_t$  where it is always positive.

$$p_t = \sqrt{p_x^2 + p_y^2} \quad (1)$$

This difference in momentum definitions may lead to further understanding of QGP and its viscosity.

### 1.2 Centrality

#### Number of Particles

In order to calculate momentum correlations, we must be able to separate the collision events according to centrality,  $b$  a measure of how close the two nuclei are to a head on collision. The impact parameter,  $b$ , is the distance between the centers of the two gold nuclei. In our calculation we bin collision events with respect to the number of particles,  $N_{part}$ , which is the

number of nucleons from both nuclei that are involved in the collision. A higher  $N_{part}$  corresponds to central collisions while low  $N_{part}$  corresponds to peripheral collisions.

## Rapidity

In this project, we use rapidity and pseudo-rapidity to represent z-momentum. Pseudo-rapidity,  $\eta$ , is a measure of the angle from the particle beam to the given particle's momentum.

$$\eta = \frac{1}{2} \ln \left( \frac{|p| + p_z}{|p| - p_z} \right) \quad (2)$$

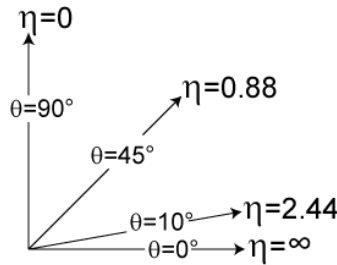


*Figure 1: This is a visual representation of  $\eta$  and its relation to the angle from the particle beam. When there is more  $p_z$ ,  $\eta$  is larger.*

Relative pseudo-rapidity,  $\Delta\eta = \eta_1 - \eta_2$ , is the difference between the rapidities of two particles and represents the amount of time two particles are communicating. A small  $\Delta\eta$  means the particles are close in momentum so they interact for the length of the collision, while large  $\Delta\eta$  means the particles only interact for a short time at the beginning of the collision. This can be very helpful later when calculating momentum correlations, which is binned by STAR<sup>2</sup> with respect to  $\Delta\eta$ . This will give some comparison to experimental values and lead to more insight into QGP viscosity.

STAR only sees  $|\eta| < 1$  although many particles are outside of this range.<sup>2</sup> This is one of the benefits of using simulated events, we can expand the acceptance parameter,  $\eta$ , and include all of the particles from the collision. This is essential as the viscosity calculation depends on the inclusion of all particles.

## 1.2 AMPT

For our calculations we took data produced by the AMPT(A Multi Phase Transport Model) simulation engine. AMPT simulates collisions with a ‘‘Parton cascade’’, like a gas of quarks and gluons. Because ref. (1) assumes hydrodynamic evolution, we expect a difference between these different methods and measurements. Due to the delicate nature of AMPT, we were able to only get 9000 collision events to run our analysis on.

## 2 Measuring Correlations

## 2.1 Transverse Momentum

We started our research by calculating the momentum covariance, in order to compare to STAR measurement<sup>2</sup> and ensure the accuracy of our calculation.  $C_{p_t p_t}$  is a standard covariance relation

$$C_{p_t p_t} = \frac{1}{\langle N \rangle^2} \left\langle \sum_{\text{pairs}} p_{ti} p_{tj} \right\rangle - \langle p_t \rangle^2 \quad (3)$$

where  $\langle N \rangle$  is the average number of particles per event. The average transverse momentum,  $\langle p_t \rangle$ , is defined as

$$\langle P_t \rangle = \frac{1}{N_{ev}} \sum_{k=1}^{N_{ev}} \sum_{i=1}^{N_k} p_{ti} \quad (4)$$

$$\langle p_t \rangle = \frac{\langle P_t \rangle}{\langle N \rangle} \quad (5)$$

In eq. (3), the first term is the sum of all the correlations between particles and the second term subtracts off all random correlations between particles. If there are no momentum correlations then  $C = 0$ .

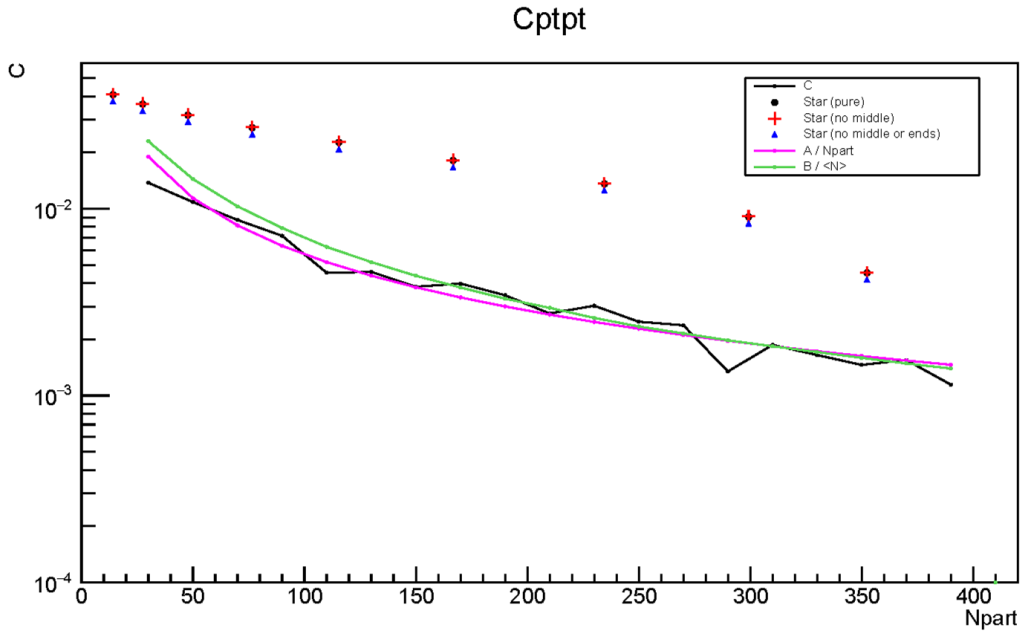


Figure 2:  $C_{p_t p_t}$  is calculated using the kinematic cuts from STAR,  $0.2 \text{ GeV} > p_t < 2 \text{ GeV}$ ,  $|\eta| < -1$ , and only charged particles.

In closer inspection,  $C_{p_t p_t}$  resembles a trend of  $\frac{A}{N_{part}}$  or  $\frac{B}{\langle N \rangle}$  as seen in fig. (2). Plotting these fits shows they come surprisingly close to  $C_{p_t p_t}$ , although only  $\frac{B}{\langle N \rangle}$  continues this trend as the rapidity range is increased.

To get the STAR points, we integrated the function below for each centrality class. The point in the middle has been claimed as an experimental error, so in addition to the pure data there is also plotted two sets of points ignoring this middle point. The first of these two makes little change to the values while the second set also ignores several points from the tails of the function which lowers the values very little.

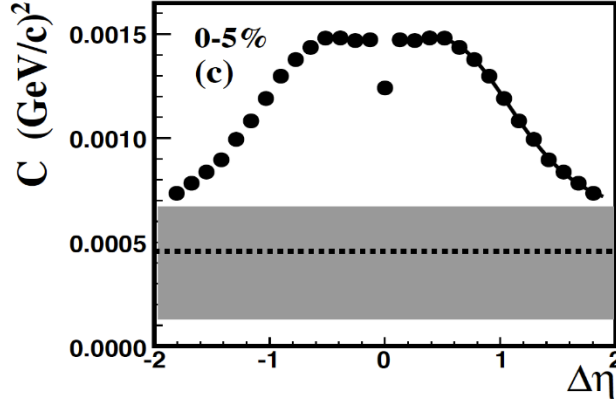


Figure 3: STAR integration of  $C$  for 0-5% centrality.

There are two reasons why the STAR data<sup>2</sup> does not line up with our calculation. AMPT might get the physics wrong and lead to this discrepancy. STAR measures  $C_{p_t p_t}$  differently than eq. (3), they measure  $C$  as in fig. (3) while we take the integral over  $\Delta\eta$  to get the points in fig. (2). This leads to the possibility that the first term of eq. (3) gives the wrong number when integrated, because taking the integral of a fraction is not the same as taking the integral of its numerator over the integral of its denominator.

$$\int \left( \frac{a}{b} \right) \neq \frac{\int a}{\int b} \quad (6)$$

This has all been calculated before and is interesting but only serves as a foundation of our understanding of  $C$  using Cartesian momentum. In order to do this we expand the rapidity cuts for the calculation until we include all particles. This is something that STAR cannot do as pointed out in Section 1.2. This is important because  $C_{p_x p_x}$ , as described in Section 2.2, should move to a limiting function as all particles are included as shown by ref. (1). In fig. (4)  $C_{p_t p_t}$  changes significantly as the rapidity cuts go to infinity. This will give us a better understanding of how  $C_{p_x p_x}$  changes when the same cuts are made.

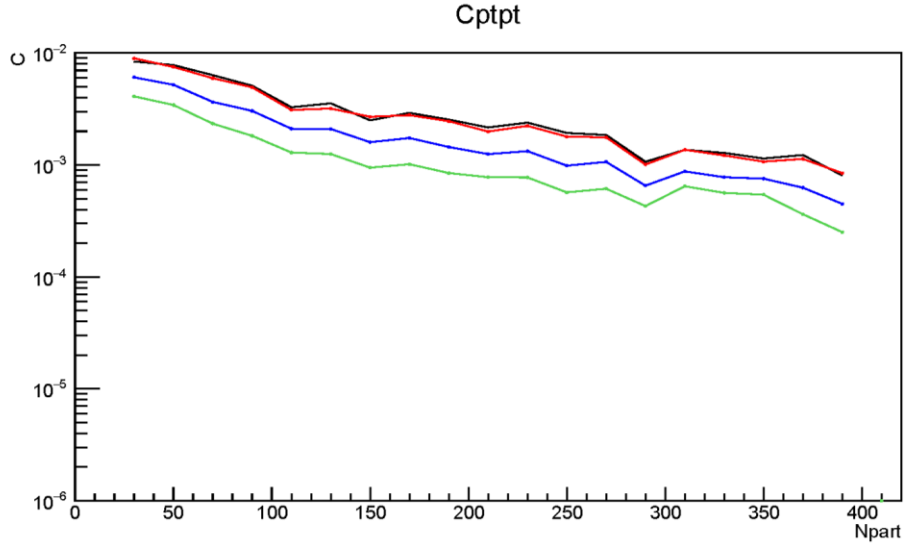


Figure 4: Different rapidity cuts of  $C_{p_t p_t}$  where  $|\eta| < 0.5$  (black),  $|\eta| < 1$  (red),  $|\eta| < 3$  (blue), and  $|\eta| < 6$  (green) are the cuts.

## 2.2 Cartesian Momentum

The Cartesian momentum covariance correlation function is identical to that for transverse other than the change of momentum.

$$C_{p_x p_x} = \frac{1}{\langle N \rangle^2} \left\langle \sum_{\text{pairs}} p_{xi} p_{xj} \right\rangle - \langle p_x \rangle^2 \quad (7)$$

The terms in this equation are the same as eq. (3), but the second term acts differently in this case. Because  $p_x$  is conserved, when you include all particles the average momentum should be zero whereas when you include all particles for the transverse covariance the average momentum does not go to zero.

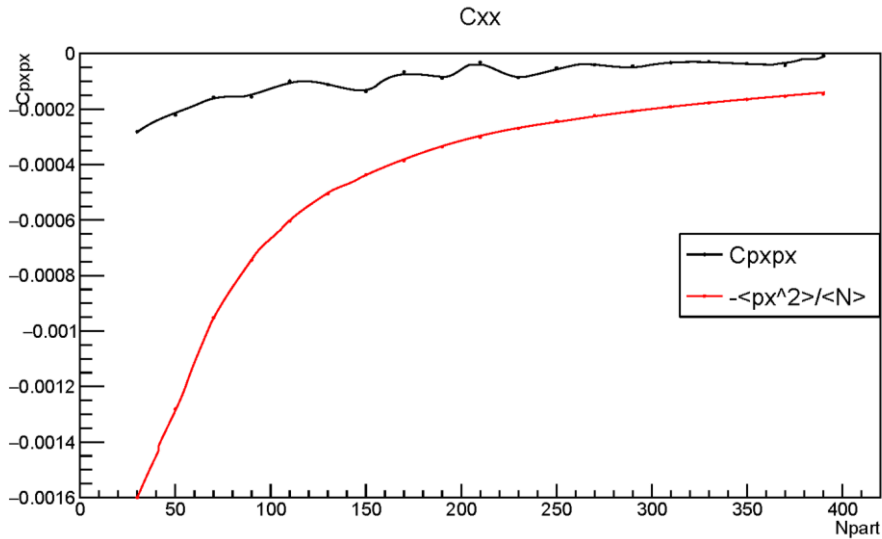


Figure 5:  $C_{p_x p_x}$  is calculated using the kinematic cuts from STAR,  $0.2 \text{ GeV} > p_t < 2 \text{ GeV}$ ,  $|\eta| < -1$ , and only charged particles.

Theoretically, as the cuts on the events increase and all particles are included  $C_{p_x p_x}$  will go toward a limiting function<sup>1</sup> of

$$C_{p_x p_x} = -\frac{\langle p_x^2 \rangle}{\langle N \rangle} \quad (8)$$

This is illustrated in Figure 5; as the rapidity cuts are increased to include all particles the right side of eq. (9) gets smaller because of the increase in  $\langle N \rangle$ . At the same time, the second term in eq. (7) goes to zero leaving only the first term which is equal to the limit in eq. (9).<sup>1</sup>

$$C_{p_x p_x} \rightarrow -\frac{\langle p_x^2 \rangle}{\langle N \rangle} \quad (9)$$

This relation can be seen in fig. (6) as the rapidity cuts are increased to include all particles. This gives more credibility to the claims made in ref. (1) concerning  $C_{p_x p_x}$ .

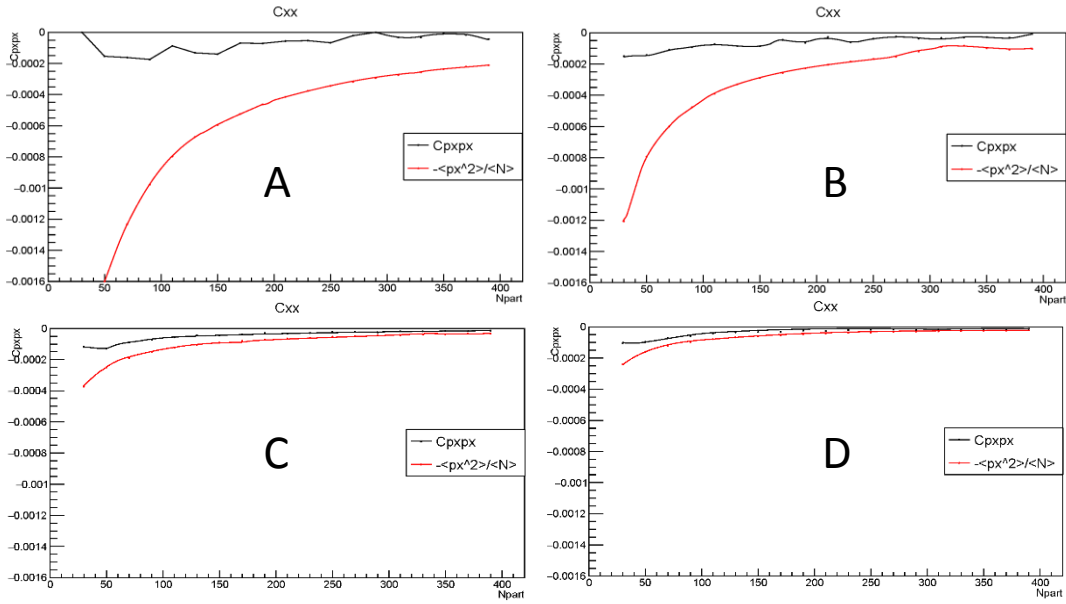


Figure 6:  $C_{p_x p_x}$  plotted against  $-\frac{\langle p_x^2 \rangle}{\langle N \rangle}$  with increasing rapidity cuts. (A)  $|\eta| < 0.5$  (B)  $|\eta| < 1$  (C)  $|\eta| < 3$  (D)  $|\eta| < 6$ .

Now that we have established  $C_{p_t p_t}$ ,  $C_{p_x p_x}$ , and how they change when the kinematic cuts are expanded, we can see that there is a definite trend. As the rapidity acceptance is increased, the magnitude of both covariance functions decreases as seen in fig. (4) and fig. (7). This will be important when we look at the viscosity with respect to transverse and Cartesian momentums.

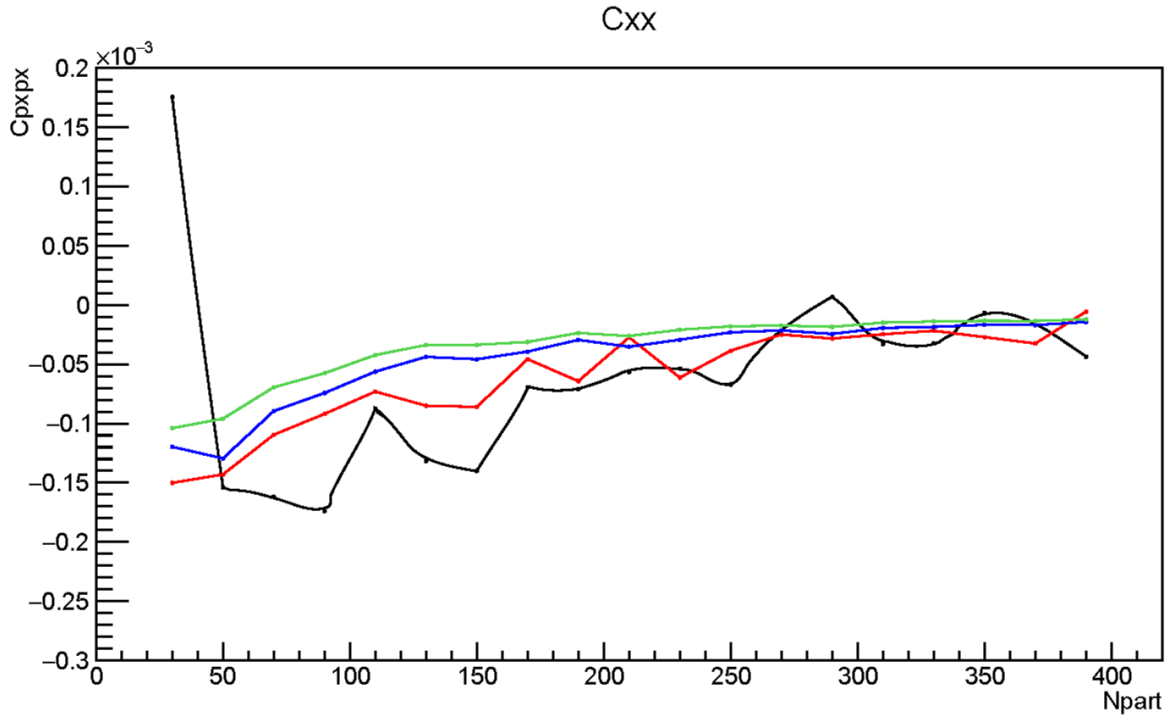


Figure 7: Different rapidity cuts of  $C_{p_x p_x}$  where  $|\eta| < 0.5$  (black),  $|\eta| < 1$  (red),  $|\eta| < 3$  (blue), and  $|\eta| < 6$  (green) are the cuts.

### 3 Conclusion

We have given  $C_{p_x p_x}$  more theoretical foundation by examining the effect of the expansion of particle inclusion from the STAR experiment window to all particles. We can use this information to measure the viscosity and other transport coefficients of QGP.<sup>1</sup>

### 4 Future

There is much left to do and many exciting paths to take in continuing this research. The most important is switching to the UrQMD simulation engine where we have access to millions of events that have been pre-generated. This will increase the accuracy and dependability of our calculations considerably.

Another path of exploration is calculating the differential momentum covariance that is given by STAR. This will allow us to look at the possible inaccuracy of Equation 4 and give us more insight into the viscosity of QGP at different centralities.

An obvious extension is to look at  $C_{p_y p_y}$  and  $C_{p_x p_y}$ . From preliminary calculations,  $C_{p_y p_y}$  acts very much like  $C_{p_x p_x}$ , while the mixed momentum covariance is still uncharted and may lead to some interesting things.

This will lead into the calculation of the viscosity of QGP and result in a paper.

## 5 Acknowledgements

I would like to thank Claude Preanu, Chris Zin, Sean Gavin, and George Moschelli for their helpful discussions and W. Llope for future help in utilizing UrQMD.

## 6 References

1. Gavin, S., Moschelli, G. & Zin, C. Rapidity Correlation Structure in Nuclear Collisions. *ArXiv160602692 Hep-Ph Physicsnucl-Th* (2016).
2. STAR Collaboration. Evolution of the differential transverse momentum correlation function with centrality in Au+Au collisions at  $\sqrt{s_{NN}} = 200$  GeV. *Phys. Lett. B* **704**, 467–473 (2011).
3. Vogt, R. Ultrarelativistic heavy-ion collisions. (2007).